Letter

Measurement of Bell-type inequalities and quantum entanglement from Λ-hyperon spin correlations at high energy colliders

Wenjie Gong,[1,*] Ganesh Parida,[2,†] Zhoudunming Tu,[3,4,‡] and Raju Venugopalan[3,§]

[1] *Department of Physics, Harvard University, Cambridge, Massachusetts 02138, USA*
[2] *Department of Physics, University of Wisconsin-Madison, Madison, Wisconsin 53706, USA*
[3] *Department of Physics, Brookhaven National Laboratory, Upton, New York 11973, USA*
[4] *Center for Frontiers in Nuclear Science, Stony Brook, New York 11794, USA*

(Received 16 August 2021; revised 6 December 2021; accepted 3 August 2022; published 15 August 2022)

Spin correlations of Λ-hyperons embedded in the QCD strings formed in high energy collider experiments provide unique insight into their locality and entanglement features. We show from general considerations that, while the Clauser-Horne-Shimony-Holt inequality is less stringent for such states, they provide a benchmark for quantum-to-classical transitions induced by varying (i) the associated hadron multiplicity, (ii) the spin of nucleons, (iii) the separation in rapidity between pairs, and (iv) the kinematic regimes accessed. These studies also enable the extraction of quantitative measures of quantum entanglement. We first explore such questions within a simple model of a QCD string composed of singlets of two partial distinguishable fermion flavors and compare analytical results to those obtained on quantum hardware. We further discuss a class of spin Hamiltonians that model the dynamics of Λ spin correlations. Prospects for extracting quantum features of QCD strings from hyperon measurements at current and future colliders are outlined.

DOI: 10.1103/PhysRevD.106.L031501

The promise of solving *ab initio* real-time many-body problems in quantum field theory motivates the interest in quantum information science (QIS) for high energy physics [1]. For instance, an outstanding problem in quantum chromodynamics (QCD) at high energies is the origin of "ridge" [2] long-range rapidity correlations which offer unique insight into the thermalization process in the quark-gluon plasma (QGP) [3]. While answers to these questions will only be obtained past the noisy intermediate scale quantum (NISQ) era, focused questions on problems universal to simpler systems can provide valuable answers sooner [4–20].

In the case of the ridge correlations, QIS studies may help identify (and classify) intrinsically quantum features such as Hanbury-Brown–Twiss and Bose-enhanced gluon correlations [21,22] arising from the entanglement of partons (quarks, antiquarks, and gluons) within an ensemble of QCD strings [23,24]. Their dynamics is presently only implemented classically in Monte Carlo (MC) generators that simulate collider events [25]. Further, quantum correlations of partons are not easily separable from those arising from their rescattering [26] with increasing density in the string ensemble. Useful lessons on such quantum-to-classical transitions may come from tabletop experiments with ultracold atomic gases [27]; a powerful example of this synergy is provided by the nonthermal fixed points universal to QGP thermalization and ultracold atomic gases [28,29].

Quantum correlations within QCD strings or string ensembles can be studied at electron-positron (e^+e^-) colliders [30], in deeply inelastic electron-proton scattering (DIS) experiments [31,32], and in hadronic collisions [33]. For example, a remarkable observation in collider data that is suggestive of the role of entanglement is the apparent thermal distribution of small numbers of produced particles in a QCD string [34,35].

In this paper, we will explore the possibility that Λ and $\bar{\Lambda}$-hyperon spin correlations provide novel insight into intrinsically quantum features of many-body parton dynamics. Such measurements are feasible because the weak decay $\Lambda \to \pi^- + p$ allows one to extract the Λ's (and analogously, that of $\bar{\Lambda}$) spin polarization to be $\mathbf{P} = \alpha\hat{\mathbf{a}}$, where $\hat{\mathbf{a}}$ denotes the direction of the daughter proton's momentum in the Λ rest frame, and $\alpha \approx 0.750$

*wenjiegong@college.harvard.edu
†parida@wisc.edu
‡zhoudunming@bnl.gov
§rajuv@bnl.gov

[36].[1] The use of Λ-hyperon spin correlations in QIS was first suggested in [38] as a test[2] of local hidden variable theory (LHVT) [42–44] by employing the Clauser-Horne-Shimony-Holt (CHSH) [45] inequality

$$|E(\hat{\mathbf{a}}, \hat{\mathbf{b}}) - E(\hat{\mathbf{a}}, \hat{\mathbf{b}}')| + |E(\hat{\mathbf{a}}', \hat{\mathbf{b}}') + E(\hat{\mathbf{a}}', \hat{\mathbf{b}})| \leq 2, \tag{1}$$

where $E(\hat{\mathbf{a}}, \hat{\mathbf{b}}) = \langle\psi|\hat{\mathbf{a}} \cdot \sigma_1 \hat{\mathbf{b}} \cdot \sigma_2|\psi\rangle$ with $\hat{\mathbf{a}}$ and $\hat{\mathbf{b}}$ corresponding to the momentum directions of the daughter particles.[3] Measured violations of the CHSH inequality imply a violation of LHVT. However, these Bell-type tests, while interesting, are unlikely to provide stronger constraints on LHVT beyond that of tabletop experiments.[4] Further, $\Lambda\bar{\Lambda}$ correlations in a QCD string reflect the dynamics of many-body mixed states for which the CHSH test in [38] is inapplicable. Nevertheless, as we will discuss, a modified CHSH inequality, and related entanglement measures, can help quantify dynamical quantum-to-classical transitions in such systems.

We will first demonstrate a general proof of a modified LHVT test for mixed states, discuss its relation to entanglement measures, and describe their possible implications for quantum-to-classical transitions. To address quantum dynamics in multiparticle production at colliders, we will first apply this framework to a simple string model and explore how hyperon correlations are washed away with increasing multiplicity. We then discuss a class of spin Hamiltonians that capture their underlying parton dynamics. Simulations of $\Lambda\bar{\Lambda}$ correlations are discussed next, with particular attention to their implementation on quantum hardware. Finally, we address experimental opportunities in extracting quantum information from measurements. The Supplemental Material provides details of these measurements [49].

Consider the two-particle correlation function (or equivalently a joint probability distribution),

$$\frac{\langle n_{\hat{\mathbf{a}}}, n_{\hat{\mathbf{b}}}\rangle}{\langle n_{\hat{\mathbf{a}}}\rangle\langle n_{\hat{\mathbf{b}}}\rangle} = \frac{P(\hat{\mathbf{a}}, \hat{\mathbf{b}})}{P(\hat{\mathbf{a}})P(\hat{\mathbf{b}})}, \tag{2}$$

where $n_{\hat{\mathbf{a}}}$ ($n_{\hat{\mathbf{b}}}$) indicates the number of daughter particles with momentum direction $\hat{\mathbf{a}}$ ($\hat{\mathbf{b}}$) measured in a single event, and $\langle\cdots\rangle$ denotes the ensemble average. The count pair in the numerator is from the same event; those in the denominator are from different events.

We now discuss a theorem that encompasses how nonlocality and entanglement manifest in Eq. (2). For simplicity, we consider spins in the $x-z$ decay plane of the Bloch sphere and assume $|\mathbf{P}| = 1$, indicating perfect discrimination between spin-up and spin-down. Thus a daughter proton (or pion) decaying along $\hat{\mathbf{a}}$ signifies a parent hyperon spin state of spin-up along $\hat{\mathbf{a}}$. The realistic determination of the spin direction is described later in the text and in the Supplemental Material [49].

The general spin state of the two spin-$\frac{1}{2}$ hyperons [with angles θ_a (θ_b) of spin directions $\hat{\mathbf{a}}$ ($\hat{\mathbf{b}}$)] relative to the z axis of the system can be represented by a density matrix $\rho_{ab} = \sum_{i=1}^{4}\sum_{j=1}^{4}\lambda_{ij}|B_i\rangle\langle B_j|$ in the Bell basis,

$$|B_1\rangle = \frac{|00\rangle + |11\rangle}{\sqrt{2}}, \qquad |B_2\rangle = \frac{|00\rangle - |11\rangle}{\sqrt{2}},$$
$$|B_3\rangle = \frac{|01\rangle + |10\rangle}{\sqrt{2}}, \qquad |B_4\rangle = \frac{|01\rangle - |10\rangle}{\sqrt{2}}, \tag{3}$$

with λ_{ij} real due to spins being in the $x-z$ plane. Computing $P(\hat{\mathbf{a}}, \hat{\mathbf{b}}) = \mathrm{Tr}(|\theta_a\rangle|\theta_b\rangle\langle\theta_a|\langle\theta_b|\rho_{ab})$ and likewise, $P(\hat{\mathbf{a}}) = \mathrm{Tr}(|\theta_a\rangle\langle\theta_a|\rho_a)$, with $\rho_a = \mathrm{Tr}_b(\rho_{ab})$, and assuming both probabilities only depend on $\theta_a - \theta_b$ (rotational invariance, which sets $\lambda_{22} = \lambda_{33}$), and $P(\hat{\mathbf{a}}, \hat{\mathbf{b}}) = P(\hat{\mathbf{b}}, \hat{\mathbf{a}})$ (which sets $\lambda_{ij} = 0$, $i \neq j$), we obtain

$$\frac{P(\hat{\mathbf{a}}, \hat{\mathbf{b}})}{P(\hat{\mathbf{a}})P(\hat{\mathbf{b}})} = 1 + (\lambda_{11} - \lambda_{44})\cos(\theta_a - \theta_b). \tag{4}$$

We therefore conclude the following:

Theorem.—A symmetric, rotationally invariant correlation function implies that the measured state ρ_{ab} is diagonal in the Bell basis, with $\lambda_{22} = \lambda_{33}$.

In the context of the generalized CHSH inequality [50,51] for mixed two-particle spin-$\frac{1}{2}$ states diagonal in the Bell basis [with $E(\hat{\mathbf{a}}, \hat{\mathbf{b}}) = E(\theta_a - \theta_b) \equiv E(\theta_{ab})$ and coplanar spin axes $\hat{\mathbf{a}}, \hat{\mathbf{a}}', \hat{\mathbf{b}}, \hat{\mathbf{b}}'$], Eq. (1) reduces to the one-parameter inequality

$$\begin{cases} |E(\theta_{ab})| \leq \mathcal{C}\left(1 - \frac{2|\theta_{ab}|}{\pi}\right), & |\theta_{ab}| \leq \frac{\pi}{2} \\ |E(\theta_{ab})| \leq \mathcal{C}\left(1 - \frac{2(\pi - |\theta_{ab}|)}{\pi}\right), & \pi/2 \leq |\theta_{ab}| \leq \pi, \end{cases} \tag{5}$$

where $\mathcal{C} = |\lambda_{44} - \lambda_{11}|$. We can obtain $E(\theta_{ab})$ from the numerator of the measured two-particle correlation function as $E(\theta_{ab}) = \frac{1}{4}(P(\hat{\mathbf{a}}, \hat{\mathbf{b}}) + P(-\hat{\mathbf{a}}, -\hat{\mathbf{b}}) - P(-\hat{\mathbf{a}}, \hat{\mathbf{b}}) - P(\hat{\mathbf{a}}, -\hat{\mathbf{b}})$, which gives

$$E(\theta_{ab}) = (\lambda_{11} - \lambda_{44})\cos(\theta_{ab}). \tag{6}$$

Comparing Eq. (6) to Eq. (5) leads us to a corollary to our theorem:

Corollary 1.—A symmetric, rotationally invariant correlation function implies that the measured state ρ_{ab}

[1] This value updates that of 0.642 quoted in Ref. [37].

[2] It was further examined in the context of e^+e^- collisions [39] and for top-quark and Higgs measurements at colliders [40,41].

[3] Note that the Pauli operator σ_i acts on particle i, and we denote spin-up as 1 and spin-down as -1.

[4] For discussions of precision LHVT tests, with emphases on potential loopholes, see [46–48].

violates its related CHSH inequality, indicating incompatibility with LHVT.

As the theorem and corollary indicate, the CHSH inequality is violated more easily for our mixed hyperon states relative to pure states. The above criteria are therefore sufficient to negate classical/deterministic explanations of their spin correlations.

In quantifying entanglement, of several possible measures [52], entanglement fidelity defined as

$$\mathcal{F}_i = \langle B_i|\rho_{ab}|B_i\rangle \equiv \lambda_{ii} \tag{7}$$

is the most straightforward to extract from measured $\Lambda\bar{\Lambda}$ spin correlations with ρ_{ab} entangled if $\mathcal{F}_i > \frac{1}{2}$. Since the coefficient of $\cos(\theta_{ab})$ in Eq. (4) is $\lambda_{11} - \lambda_{44}$, we obtain a second corollary to our theorem:

Corollary 2.—If the magnitude of the coefficient of $\cos(\theta_{ab})$ in a symmetric rotationally invariant correlation function is $> \frac{1}{2}$, then the measured state ρ_{ab} is entangled.

The criterion $\mathcal{F}_i > \frac{1}{2}$ is sufficient but not necessary for entanglement. A necessary and sufficient entanglement measure, albeit more challenging to extract at colliders, is the Peres-Horodecki positive partial transpose (PPT) criterion [53,54]; it is discussed at length in the Supplemental Material [49].

Our theorem and corollaries provide a novel approach to quantifying quantum-to-classical transitions in many-body systems. For example, the aforementioned ridge effect for $\Lambda\bar{\Lambda}$ correlations could arise from hydrodynamic flow (the LHVT) in high multiplicity events. As we would anticipate, rotational invariance of the correlations is broken because of a preferred "reaction plane" in such events. The converse, a quantum effect that breaks rotational invariance, is feasible; however, since microscopic interactions in QCD respect rotational invariance, its observed violation with increasing multiplicity signals onset of a quantum-to-classical transition.

To flesh out these general results, and in particular ascertain the role of entanglement, we will first consider a very simple spin model for Λ-hyperons embedded in a QCD string. Here heavy strange-antistrange quarks ($s\bar{s}$) are mixed up with light parton pairs of one other flavor $u\bar{u}$ along the QCD string. Hadronization in this picture corresponds to the parton ensemble of $s, \bar{s}, u$, and $\bar{u}$ being grouped, after hadronization, into spin singlets with possible singlet combinations[5] being $s\bar{s}$, $u\bar{s}$, $s\bar{u}$, and $u\bar{u}$. For N partons, there are a singlets of type $s\bar{s}$, $b/2$ singlets of type $s\bar{u}$, $b/2$ singlets of type $u\bar{s}$, and $N/2 - a - b$ singlets of type $u\bar{u}$. Hence there are $2a + b$ particles of type s or $\bar{s}$ and $N - 2a - b$ particles of type u or $\bar{u}$. We assume the ground state wave function of parton singlets corresponds to their occupying the lowest $N/2$ energy levels of the string, with $s\bar{s}$ on levels $1...a$, $s\bar{u}$ on levels $a+1...a+b/2$, $u\bar{s}$ on levels $a+b/2+1...a+b$, and $u\bar{u}$ on levels $a+b+1...N/2$; the relevant aspect for us is the orthogonality of individual wave functions.

The explicit computation of $s\bar{s}$, $s\bar{u}$, and $u\bar{u}$ correlations is worked out in the Supplemental Material [49]; for the $s\bar{s}$ ($\Lambda\bar{\Lambda}$) correlations,

$$\frac{P(|\hat{n}_1\rangle, |\hat{n}_2\rangle)}{P(|\hat{n}_1\rangle)P(|\hat{n}_2\rangle)} = 1 - \frac{a}{(a+b/2)^2}\cos(\theta_2 - \theta_1). \tag{8}$$

This result depends on a and b since they are the only parameters that determine the number of $s\bar{s}$, $s\bar{u}$, and $u\bar{s}$ singlets. It clearly violates the CHSH inequality for mixed states for all values of a and b. The coefficient of the cosine is plotted for various a and b in Fig. 1. As may be anticipated, adding mixed singlets, or having $b > 0$, decreases the entanglement fidelity since their indistinguishability washes out the spin correlation. The corresponding PPT entanglement criterion for this model is discussed in the Supplemental Material [49].

Our toy model shows that, even though entanglement fidelity is washed away, nonlocality can persist; for locality to emerge necessitates further many-body interactions that break rotational invariance, generating classical correlations.

QIS discussions of stringy phenomena are dominantly in the Schwinger model and its variants [34,35]. However, since $\Lambda\bar{\Lambda}$ correlations are a promising probe of quantum features of strings, models where heavy strange quarks interact with light up/down quarks provide novel insight. A good starting point is the Anderson model of localized impurities coupled to delocalized fermion spins [55],

$$H_{\text{Anderson}} = \sum_{k\sigma}\epsilon_k a^\dagger_{k\sigma}a_{k\sigma} + \epsilon_d d^\dagger_\sigma d_\sigma + U d^\dagger_\uparrow d_\uparrow d^\dagger_\downarrow d_\downarrow + \frac{\eta}{\sqrt{V}}(d^\dagger_\sigma a_{k\sigma} + a^\dagger_{k\sigma}d_\sigma). \tag{9}$$

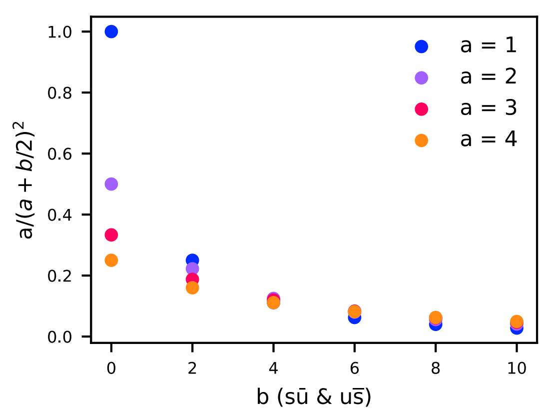

FIG. 1. The coefficient $\frac{a}{(a+b/2)^2}$ in Eq. (8) plotted for various a and b corresponding to $s\bar{s}$ and $u\bar{s}(s\bar{u})$ pairs in the string. A coefficient greater than $\frac{1}{2}$ satisfies the entanglement fidelity criterion.

[5]These are proxies for $\Lambda\bar{\Lambda}$, kaon, and pion states, respectively; up and down quark pairs are taken as indistinguishable.

Here the $d_\sigma^\dagger(d_\sigma)$'s denote the localized impurities with spins σ (denoting heavy strange quarks carrying Λ spin [56,57]) and the $a_\sigma^\dagger(a_\sigma)$'s represent the delocalized fermions (light up and down quarks); the first two terms in the Hamiltonian are their respective kinetic energies. The third term is a Hubbard-type hopping term for the light quarks and the final term denotes their spin coupling to the strange quark impurities. This last term "screens" the formation of $\Lambda\bar{\Lambda}$ singlets. A Schrieffer-Wolff transformation [58], with the impurity kinetic energy ϵ_d below the Fermi energy recovers the Kondo Hamiltonian, describing the net spin coupling of delocalized fermions to the impurity spin $\mathbf{S}$.

Further insight into correlations between the $\Lambda\bar{\Lambda}$ pairs "doping" the QCD string is obtained in an extension of the Kondo model,[6] whose ground state is a filled Fermi sea of light fermions and impurities, with additional phase factors denoting their spatial locations. Eliminating excitations of the Fermi sea via another Schrieffer-Wolff transformation results in an effective Hamiltonian of localized impurities with interactions mediated by the exchange of virtual electron-hole pairs.

This Ruderman-Kittel-Kasuya-Yoshida (RKKY) effective Hamiltonian [60–62] mimics the QCD string at small values of the DIS Bjorken x variable, where a large multiplicity of light quark/gluon pairs either screen or antiscreen the correlations between Λ-hyperons, taking the form

$$H_{\mathrm{RKKY}} = \sum_{jj'} \mathbf{S}_j \cdot \mathbf{S}_{j'} J_{\mathrm{RKKY}}(R_j - R_{j'}), \qquad (10)$$

with

$$J_{\mathrm{RKKY}}(R) = \frac{-J^2}{(k_F R)^4}[\sin(2k_F R) - 2k_F R\cos(2k_F R)],$$

where k_F is the Fermi momentum. It is ferromagnetic at short distances but has alternating sign at larger distances, suggestive of glassy dynamics.

While the RKKY model is a good model of $\Lambda\bar{\Lambda}$ correlations for small x, a better fit for the "impurity doped" QCD string at large x is the Anderson model with multiple impurities [63]. In analogy to a quantum phase transition proposed [64] between Kondo and RKKY regimes, it would be interesting to investigate consequences of the increased multiplicity of QCD strings with varying Bjorken x. In polarized DIS, valence quark spin plays an analogous role to a magnetic field providing an additional handle on simulating string dynamics. Thus mapping the rich dynamics of the Anderson/Kondo model, "tuned" appropriately to measurements of $\Lambda\bar{\Lambda}$ correlations embedded in QCD strings, offers a novel direction in QIS studies of hadronization at colliders.

[6] See [59] for a similar discussion of heavy flavor impurities in quark matter at high baryon densities.

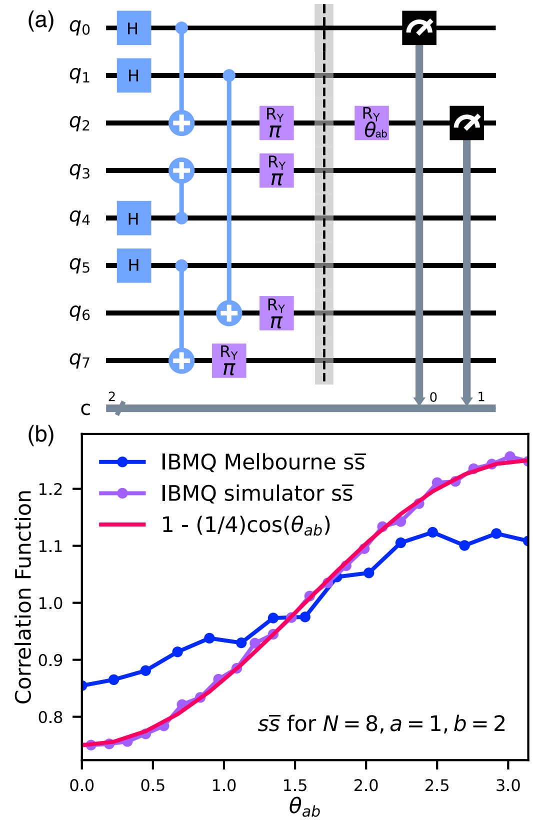

FIG. 2. (a) One of 16 circuits necessary to initialize and simulate the state of $N = 8$ particles with $a = 1$ $s\bar{s}$ singlets, $b = 2$ $s\bar{u}$ and $u\bar{s}$ singlets, and one $u\bar{u}$ singlet. Here, each qubit q_i carries the spin information of one of the $N = 8$ particles, while the classical register c stores the value of the qubit obtained after measurement. The barrier separates initialization from simulation of the correlation function. (b) Quantum simulation results for the $s\bar{s}$ correlation function compared to the prediction in Eq. (8). Correlations obtained from the IBM Q Melbourne quantum computer are smaller than our analytical calculation due to quantum hardware noise; this hardware error will pose even greater restrictions for simulations of larger ensembles N.

There are several classical approaches to simulating the ground state properties of the aforementioned spin Hamiltonians [63,65–68]. However, such Hamiltonians suffer from a severe dynamical sign problem that afflicts the extraction of real-time correlations [69]. Since the formation, evolution, and fragmentation of QCD strings are dynamical real-time problems, they are susceptible to the sign problem even in lower-dimensional incarnations.

Quantum computers do not suffer from this problem, with benchmark computations performed for the Ising model in an external magnetic field [70]. The quantum computation of Anderson and Kondo lattices has been discussed previously [71]; digital simulations of these Hamiltonians, adapted to the QCD string, are in progress.

As a first step, we wrote down quantum circuits for our toy model and performed computations on IBM's QISKIT quantum simulator [72] and on IBM Q quantum hardware,

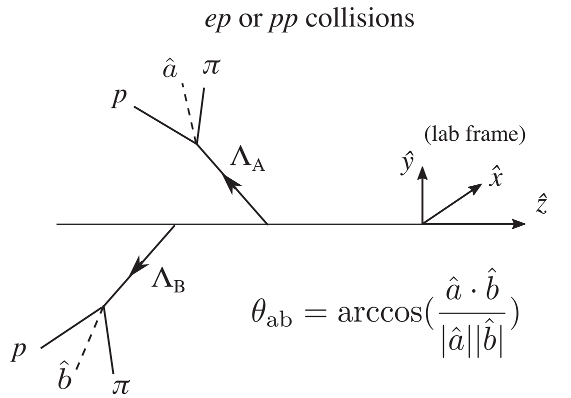

FIG. 3. Illustration of double Λ polarization; here $\hat{a}$ ($\hat{b}$) denotes the momentum direction of Λ_A (Λ_B) daughter particle in the Λ_A (Λ_B) rest frame.

specifically ibmq_16_melbourne containing 14 qubits [73]. This computation is outlined in the Supplemental Material [49]. In Fig. 2(a), we show one of the 16 circuits necessary to generate and simulate the mixed spin density matrix for the case of $N = 8$ spin-$1/2$ fermions, with $a = 1$ (one $s\bar{s}$ pair), $b = 2$ (one $s\bar{u}$ and $\bar{s}u$ singlet each), and $N/2 - a - b$, one $u\bar{u}$ singlet. In Fig. 2(b), we show the analytical result from Eq. (8) compared to the result from the QISKIT simulator; we find good agreement. In contrast, the agreement with actual quantum hardware is not good, illustrating the challenge of reliable quantum simulation in the NISQ era.

Finally, we discuss the experimental opportunities in measuring $\Lambda\bar{\Lambda}$ correlations at colliders. The Λ and $\bar{\Lambda}$ spins are measured in terms of their polarization, where the decay kinematics on an event-averaged basis reflects their spin projections [74–87]. The CHSH inequality and entanglement measures are extracted from the correlation of their relative spin projections, illustrated in Fig. 3 and written as $N \propto 1 + \alpha^2 P_{\Lambda,\Lambda} \cos(n\theta_{\rm ab})$, where n is a free parameter that can be determined by the measurement and is expected to be less than unity due to a convolution between the intrinsic CHSH cosine modulation and the Λ decay kinematics.[7] As noted, $\alpha = 0.750 \pm 0.010$ [36], $\theta_{\rm ab}$ is the relative angle between daughter particles in their respective mother's rest frame, and a nonzero $P_{\Lambda,\Lambda}$ implies their spin correlation.

Currently, no MC generators implement spin entanglement at the parton level, providing a clear (null result) experimental baseline for entanglement searches. Specifically, we can simulate "by hand" spin entanglement in the PYTHIA 8 MC event generator [88]; the Supplemental Material discusses in detail simulation results and experimental measurements [49].

In summary, we derived in this paper a modification of the CHSH inequality, and related entanglement measures, for mixed states. These are powerful tools in quantifying quantum-to-classical transitions in the many-body dynamics of strings in the collider environment. We further constructed theoretical models to capture the quantum dynamics of QCD strings with embedded hyperons and discussed how these can be extracted from $\Lambda\bar{\Lambda}$ correlations. With a longer term view of QIS, we performed first simulations on quantum hardware; these provide a benchmark and illustrate the current challenges in reliable extraction of quantum information. Further systematic studies implementing quantum error correction, state preparation, Trotter evolution, and entanglement measures will be reported separately. MC simulations of Λ correlation measurements at colliders suggest that prospects for extracting information on quantum-to-classical transitions in QCD strings are promising.

We thank Robert Konik for discussions on spin Hamiltonians, Elke-Caroline Aschenauer for discussions on spin polarization measurements, and Alexander Jentsch for discussions of Λ particle detection in the far-forward region at the EIC. We acknowledge the use of IBM Quantum services for this work. The views expressed are those of the authors, and do not reflect the official policy or position of IBM or the IBM Quantum team. The work of W. G. is supported in part by the U.S. Department of Energy, Office of Science, Office of Workforce Development for Teachers and Scientists (WDTS) under the Science Undergraduate Laboratory Internships Program (SULI). Access to IBM's quantum hardware is provided through Harvard University and Brookhaven National Laboratory's Scientific Data and Computing Center (SDCC). The work of G. P. was supported in part by the S. N. Bose Scholars Program, jointly funded by the Government of India [Department of Science and Technology (DST)—Science and Engineering Board (SERB)], Indo-U.S. Science and Technology Forum (IUSSTF), and WINStep Forward and in part by the U.S. Department of Energy under Award No. DE-SC0012704. The work of Z. T. is supported by LDRD-039 and the Goldhaber Distinguished Fellowship at Brookhaven National Laboratory. Z. T. and R. V. are supported by the U.S. Department of Energy under Award No. DE-SC0012704. The work of W. G. and R. V. on quantum information science is supported in part by the U.S. Department of Energy, Office of Science National Quantum Information Science Research Center's Co-design Center for Quantum Advantage ($\mathrm{C^2QA}$) under Award No. DE-SC0012704.

[7]The cosine modulation in Eq. (8) and in Λ decays are of different origin.

[1] J. Preskill, Simulating quantum field theory with a quantum computer, Proc. Sci., LATTICE2018 (**2018**) 024 [arXiv:1811.10085], https://pos.sissa.it/334/024.
[2] V. Khachatryan *et al.* (CMS Collaboration), Observation of long-range, near-side angular correlations in proton-proton collisions at the LHC, J. High Energy Phys. 09 (2010) 091.
[3] J. Berges, M. P. Heller, A. Mazeliauskas, and R. Venugopalan, QCD thermalization: Ab initio approaches and interdisciplinary connections, Rev. Mod. Phys. **93**, 035003 (2021).
[4] S. R. Beane, D. B. Kaplan, N. Klco, and M. J. Savage, Entanglement Suppression and Emergent Symmetries of Strong Interactions, Phys. Rev. Lett. **122**, 102001 (2019).
[5] N. Mueller, A. Tarasov, and R. Venugopalan, Deeply inelastic scattering structure functions on a hybrid quantum computer, Phys. Rev. D **102**, 016007 (2020).
[6] H. Lamm, S. Lawrence, and Y. Yamauchi (NuQS Collaboration), Parton physics on a quantum computer, Phys. Rev. Research **2**, 013272 (2020).
[7] B. Chakraborty, M. Honda, T. Izubuchi, Y. Kikuchi, and A. Tomiya, Digital quantum simulation of the Schwinger model with topological term via adiabatic state preparation, Phys. Rev. D **105**, 094503 (2022).
[8] D. E. Kharzeev and Y. Kikuchi, Real-time chiral dynamics from a digital quantum simulation, Phys. Rev. Research **2**, 023342 (2020).
[9] M. Kreshchuk, W. M. Kirby, G. Goldstein, H. Beauchemin, and P. J. Love, Quantum simulation of quantum field theory in the light-front formulation, Phys. Rev. A **105**, 032418 (2022).
[10] J. Liu and Y. Xin, Quantum simulation of quantum field theories as quantum chemistry, J. High Energy Phys. 12 (2020) 011.
[11] R. A. Briceño, J. V. Guerrero, M. T. Hansen, and A. M. Sturzu, Role of boundary conditions in quantum computations of scattering observables, Phys. Rev. D **103**, 014506 (2021).
[12] Z. Davoudi, I. Raychowdhury, and A. Shaw, Search for efficient formulations for Hamiltonian simulation of non-Abelian lattice gauge theories, Phys. Rev. D **104**, 074505 (2021).
[13] W. A. de Jong, K. Lee, J. Mulligan, M. Płoskoń, F. Ringer, and X. Yao, Quantum simulation of non-equilibrium dynamics and thermalization in the Schwinger model, arXiv:2106.08394.
[14] E. Gustafson, Y. Zhu, P. Dreher, N. M. Linke, and Y. Meurice, Real-time quantum calculations of phase shifts using wave packet time delays, Phys. Rev. D **104**, 054507 (2021).
[15] J. a. Barata, N. Mueller, A. Tarasov, and R. Venugopalan, Single-particle digitization strategy for quantum computation of a ϕ^4 scalar field theory, Phys. Rev. A **103**, 042410 (2021).
[16] J. a. Barata and C. A. Salgado, A quantum strategy to compute the jet quenching parameter $\hat{q}$, Eur. Phys. J. C **81**, 862 (2021).
[17] T. Li, X. Guo, W. K. Lai, X. Liu, E. Wang, H. Xing, D.-B. Zhang, and S.-L. Zhu, Partonic Structure by Quantum Computing, Phys. Rev. D **105**, L111502 (2022).
[18] M. Honda, E. Itou, Y. Kikuchi, L. Nagano, and T. Okuda, Digital quantum simulation for screening and confinement in gauge theory with a topological term, Phys. Rev. D **105**, 014504 (2022).
[19] K. Ikeda, D. E. Kharzeev, and Y. Kikuchi, Real-time dynamics of Chern-Simons fluctuations near a critical point, Phys. Rev. D **103**, L071502 (2021).
[20] N. Klco and M. J. Savage, Entanglement Spheres and a UV-IR Connection in Effective Field Theories, Phys. Rev. Lett. **127**, 211602 (2021).
[21] A. Dumitru, K. Dusling, F. Gelis, J. Jalilian-Marian, T. Lappi, and R. Venugopalan, The ridge in proton-proton collisions at the LHC, Phys. Lett. B **697**, 21 (2011).
[22] A. Kovner and V. V. Skokov, Bose enhancement, the Liouville effective action and the high multiplicity tail in p-A collisions, Phys. Rev. D **98**, 014004 (2018).
[23] J. B. Kogut and L. Susskind, Hamiltonian formulation of Wilson's lattice gauge theories, Phys. Rev. D **11**, 395 (1975).
[24] G. S. Bali, QCD forces and heavy quark bound states, Phys. Rep. **343**, 1 (2001).
[25] B. Andersson, G. Gustafson, G. Ingelman, and T. Sjostrand, Parton fragmentation and string dynamics, Phys. Rep. **97**, 31 (1983).
[26] K. Dusling, W. Li, and B. Schenke, Novel collective phenomena in high-energy proton-proton and proton-nucleus collisions, Int. J. Mod. Phys. E **25**, 1630002 (2016).
[27] B. Luca, M. Holten, R. Klemt, K. Subramanian, J. Bjerlin, S. M. Reimann, G. M. Bruun, P. M. Preiss, and S. Jochim, Observing the emergence of a quantum phase transition shell by shell, Nature (London) **587**, 583 (2020).
[28] J. Berges, K. Boguslavski, S. Schlichting, and R. Venugopalan, Universality far from Equilibrium: From Superfluid Bose Gases to Heavy-Ion Collisions, Phys. Rev. Lett. **114**, 061601 (2015).
[29] M. Prüfer, P. Kunkel, H. Strobel, S. Lannig, D. Linnemann, C.-M. Schmied, J. Berges, T. Gasenzer, and M. K. Oberthaler, Observation of universal dynamics in a spinor Bose gas far from equilibrium, Nature (London) **563**, 217 (2018).
[30] Y.-C. Chen, C.-W. Lin, Y.-J. Lee, and P. Chang (Belle Collaboration), Search for long range flow-like correlation in hadronic e^+e^- collisions with Belle, *Proc. Sci.*, ICHEP2020 (2021) 541.
[31] V. Andreev *et al.* (H1 Collaboration), Measurement of charged particle multiplicity distributions in DIS at HERA and its implication to entanglement entropy of partons, Eur. Phys. J. C **81**, 212 (2021).
[32] Z. Tu (H1 and ZEUS Collaboration), HERA data on azimuthal decorrelation and charged particle multiplicity spectra probing QCD dynamics and quantum entanglement effects, Proc. Sci., ICHEP2020 (**2021**) 513, https://pos.sissa.it/390/513.
[33] Z. Tu, D. E. Kharzeev, and T. Ullrich, Einstein-Podolsky-Rosen Paradox and Quantum Entanglement at Subnucleonic Scales, Phys. Rev. Lett. **124**, 062001 (2020).
[34] J. Berges, S. Floerchinger, and R. Venugopalan, Thermal excitation spectrum from entanglement in an expanding quantum string, Phys. Lett. B **778**, 442 (2018).
[35] J. Berges, S. Floerchinger, and R. Venugopalan, Dynamics of entanglement in expanding quantum fields, J. High Energy Phys. 04 (2018) 145.

[36] M. Ablikim *et al.* (BESIII Collaboration), Polarization and entanglement in baryon-antibaryon pair production in electron-positron annihilation, Nat. Phys. **15**, 631 (2019).
[37] E. Commins and P. Bucksbaum, *Weak Interactions of Leptons and Quarks* (Cambridge University Press, Cambridge, UK, 1983).
[38] N. A. Tornqvist, Suggestion for Einstein-Podolsky-Rosen experiments using reactions like $e^+e^- \to \Lambda\bar{\Lambda} \to \pi^- p \pi^+ \bar{p}$, Found. Phys. **11**, 171 (1981).
[39] X.-Q. Hao, H.-W. Ke, Y.-B. Ding, P.-N. Shen, and X.-Q. Li, Testing the Bell inequality at experiments of high energy physics, Chin. Phys. C **34**, 1 (2010).
[40] A. Barr, Testing Bell inequalities in Higgs boson decays, Phys. Lett. B **825**, 136866 (2022).
[41] M. Fabbrichesi, R. Floreanini, and G. Panizzo, Testing Bell Inequalities at the LHC with Top-Quark Pairs, Phys. Rev. Lett. **127**, 161801 (2021).
[42] D. Bohm, A suggested interpretation of the quantum theory in terms of hidden variables. 1., Phys. Rev. **85**, 166 (1952).
[43] D. Bohm, A suggested interpretation of the quantum theory in terms of hidden variables. 2., Phys. Rev. **85**, 180 (1952).
[44] A. Einstein, B. Podolsky, and N. Rosen, Can quantum-mechanical description of physical reality be considered complete?, Phys. Rev. **47**, 777 (1935).
[45] J. F. Clauser, M. A. Horne, A. Shimony, and R. A. Holt, Proposed Experiment to Test Local Hidden-Variable Theories, Phys. Rev. Lett. **23**, 880 (1969).
[46] M. Giustina *et al.*, Significant-Loophole-Free Test of Bell's Theorem with Entangled Photons, Phys. Rev. Lett. **115**, 250401 (2015).
[47] B. Hensen, H. Bernien, A. E. Dréau, A. Reiserer, N. Kalb, M. S. Blok, J. Ruitenberg, R. F. L. Vermeulen, R. N. Schouten, C. Abellán, W. Amaya, V. Pruneri, M. W. Mitchell, M. Markham, D. J. Twitchen, D. Elkouss, S. Wehner, T. H. Taminiau, and R. Hanson, Loophole-free Bell inequality violation using electron spins separated by 1.3 kilometres, Nature (London) **526**, 682 (2015).
[48] D. Rauch, J. Handsteiner, A. Hochrainer, J. Gallicchio, A. S. Friedman, C. Leung, B. Liu, L. Bulla, S. Ecker, F. Steinlechner, R. Ursin, B. Hu, D. Leon, C. Benn, A. Ghedina, M. Cecconi, A. H. Guth, D. I. Kaiser, T. Scheidl, and A. Zeilinger, Cosmic Bell Test Using Random Measurement Settings from High-Redshift Quasars, Phys. Rev. Lett. **121**, 080403 (2018).
[49] See Supplemental Material at http://link.aps.org/supplemental/10.1103/PhysRevD.106.L031501 for details of Positive Partial Transpose (PPT) criterion (Sec. 1), 2 flavors of spin chain model (Sec. 2), implementation of 2 flavors of spin chain model on the IBM Quantum Computer (Sec. 3), and experimental perspectives in high energy experiments (Sec. 4).
[50] X. H. Wu, H. S. Zong, H. R. Pang, and F. Wang, Bell inequality for Werner states, Phys. Rev. A **64**, 3 (2001).
[51] V. A. Andreev and V. I. Man'ko, Bell's inequality for two-particle mixed spin states, Theor. Math. Phys. **140**, 1135 (2004).
[52] M. B. Plenio and S. Virmani, An introduction to entanglement measures, Quantum Inf. Comput. **7**, 1 (2007).
[53] A. Peres, Separability Criterion for Density Matrices, Phys. Rev. Lett. **77**, 1413 (1996).
[54] P. Horodecki, Separability criterion and inseparable mixed states with positive partial transposition, Phys. Lett. A **232**, 333 (1997).
[55] J. Keeling, Lectures on Quantum Magnetism, https://www.st-andrews.ac.uk/~jmjk/keeling/teaching/magnetism-notes.pdf.
[56] M. Burkardt and R. L. Jaffe, Polarized $q \to \Lambda$ Fragmentation Functions from $e^+e^- \to \Lambda + X^*$, Phys. Rev. Lett. **70**, 2537 (1993).
[57] A. Moretti (COMPASS Collaboration), Transversity and Λ polarization at COMPASS, Proc. Sci., SPIN2018 (**2018**) 138 [arXiv:1901.01735].
[58] J. R. Schrieffer and P. A. Wolff, Relation between the Anderson and Kondo Hamiltonians, Phys. Rev. **149**, 491 (1966).
[59] K. Hattori, K. Itakura, S. Ozaki, and S. Yasui, QCD Kondo effect: Quark matter with heavy-flavor impurities, Phys. Rev. D **92**, 065003 (2015).
[60] M. A. Ruderman and C. Kittel, Indirect exchange coupling of nuclear magnetic moments by conduction electrons, Phys. Rev. **96**, 99 (1954).
[61] T. Kasuya, Theory of metallic ferro- and antiferromagnetism on Zener's model, Prog. Theor. Phys. **16**, 45 (1956).
[62] K. Yoshida, Magnetic properties of Cu-Mn alloys, Phys. Rev. **106**, 893 (1957).
[63] R. Žitko and J. Bonča, Multiple-impurity Anderson model for quantum dots coupled in parallel, Phys. Rev. B **74**, 045312 (2006).
[64] F. Eickhoff and F. B. Anders, Strongly correlated multi-impurity models: The crossover from a single-impurity problem to lattice models, Phys. Rev. B **102**, 205132 (2020).
[65] K. Wilson, The renormalization group: Critical phenomena and the Kondo problem, Rev. Mod. Phys. **47**, 773 (1975).
[66] H. R. Krishna-Murthy, J. W. Wilkins, and K. Wilson, Renormalization-group approach to the Anderson model of dilute magnetic alloys. I. Static properties for the symmetric case, Phys. Rev. B **21**, 1003 (1980).
[67] P. D. Sacramento and P. Schlottmann, Thermodynamics of the single-channel Kondo impurity of spin $s(\leq (7/2)$ in a magnetic field, Phys. Rev. B **40**, 431 (1989).
[68] P. W. Anderson, A poor man's derivation of scaling laws for the Kondo problem, J. Phys. C **3**, 2436 (1970).
[69] G. Cohen, E. Gull, D. R. Reichman, and A. J. Millis, Taming the Dynamical Sign Problem in Real-Time Evolution of Quantum Many-Body Problems, Phys. Rev. Lett. **115**, 266802 (2015).
[70] A. Smith, M. S. Kim, F. Pollmann, and J. Knolle, Simulating quantum many-body dynamics on a current digital quantum computer, npj Quantum Inf. **5**, 106 (2019).
[71] J. J. García-Ripoll, E. Solano, and M. A. Martin-Delgado, Quantum simulation of Anderson and Kondo lattices with superconducting qubits, Phys. Rev. B **77**, 024522 (2008).
[72] A. Asfaw *et al.*, Learn quantum computation using QISKIT (2020), https://qiskit.org/textbook/preface.html.
[73] IBM Quantum, https://quantum-computing.ibm.com (2021).
[74] Y. Guan *et al.* (Belle Collaboration), Observation of Transverse $\Lambda/\bar{\Lambda}$ Hyperon Polarization in e^+e^- Annihilation at Belle, Phys. Rev. Lett. **122**, 042001 (2019).

[75] G. Bunce *et al.*, Lambda0 Hyperon Polarization in Inclusive Production by 300-GeV Protons on Beryllium., Phys. Rev. Lett. **36**, 1113 (1976).

[76] K. J. Heller *et al.*, Polarization of Lambdas and anti-Lambdas Produced by 400-GeV Protons, Phys. Rev. Lett. **41**, 607 (1978); **45**, 1043(E) (1980).

[77] A. N. Aleev *et al.* (BIS-2 Collaboration), Polarization of Λ^0 produced by neutrons with an energy of approximately 40-{GeV} on carbon nuclei, Sov. J. Nucl. Phys. **37**, 880 (1983).

[78] P. Astier *et al.* (NOMAD Collaboration), Measurement of the Lambda polarization in nu/mu charged current interactions in the NOMAD experiment, Nucl. Phys. **B588**, 3 (2000).

[79] P. Astier *et al.* (NOMAD Collaboration), Measurement of the anti-Lambda polarization in muon-neutrino charged current interactions in the NOMAD experiment, Nucl. Phys. **B605**, 3 (2001).

[80] J. Felix *et al.* (E690 Collaboration), Λ^0 Polarization in 800 GeV/c $pp \to p_f(\Lambda^0 K^+)$, Phys. Rev. Lett. **88**, 061801 (2002).

[81] M. I. Adamovich *et al.* (WA89 Collaboration), A measurement of Λ polarization in inclusive production by Σ^- of 340-GeV/c in C and Cu targets, Eur. Phys. J. C **32**, 221 (2004).

[82] I. Abt *et al.* (HERA-B Collaboration), Polarization of Lambda and anti-Lambda in 920-GeV fixed-target proton-nucleus collisions, Phys. Lett. B **638**, 415 (2006).

[83] J. L. Sanchez-Lopez *et al.* (SELEX Collaboration), Polarization of Λ^0 and $\bar{\Lambda}^0$ inclusively produced by 610-GeV/c Σ^- and 525-GeV/c proton beams, arXiv:0706.3660.

[84] G. Agakishiev *et al.* (HADES Collaboration), Lambda hyperon production and polarization in collisions of p(3.5 GeV) + Nb, Eur. Phys. J. A **50**, 81 (2014).

[85] A. Airapetian *et al.* (HERMES Collaboration), Transverse polarization of Λ and $\bar{\Lambda}$ hyperons in quasireal photoproduction, Phys. Rev. D **76**, 092008 (2007).

[86] F. Hauenstein *et al.* (COSY-TOF Collaboration), Measurement of polarization observables of the associated strangeness production in proton proton interactions, Eur. Phys. J. A **52**, 337 (2016).

[87] L. Adamczyk *et al.* (STAR Collaboration), Global Λ hyperon polarization in nuclear collisions: Evidence for the most vortical fluid, Nature (London) **548**, 62 (2017).

[88] T. Sjöstrand, S. Mrenna, and P. Z. Skands, A brief introduction to PYTHIA8.1, Comput. Phys. Commun. **178**, 852 (2008).